

5th CIRP Global Web Conference Research and Innovation for Future Production

## On the relationship between cutting temperature and workpiece polymer degradation during CFRP edge trimming

Kevin Kerrigan<sup>a</sup> and Garret E. O'Donnell<sup>b</sup> \*

<sup>a</sup>Advanced Manufacturing Research Centre with Boeing, University of Sheffield, United Kingdom

<sup>b</sup>Department of Mechanical and Manufacturing Engineering, Trinity College Dublin, Ireland

\* Corresponding author. Tel.: +44-114-222-4839 ; fax: +44-114-222-7678. E-mail address: [k.kerrigan@amrc.co.uk](mailto:k.kerrigan@amrc.co.uk)

### 1. Abstract

This research aims to investigate thermal effects generated during conventional CNC machining of polymer-based composites. A sensorised cutting tool incorporating a wireless embedded thermocouple is used to extract tool-side temperature information during edge trimming of carbon fibre reinforced polymer (CFRP) laminates whilst an infrared thermal imaging camera extracted workpiece temperature. Force data was collected to measure the specific cutting energy for each set of parameters tested. Parameters varied included feed rate, workpiece thickness and vertical cutting strategy in conjunction with design of experiment (DOE) methods. The temperature results of this investigation indicate that both vertical cutting strategy and depth of cut produce strongly significant effects on the steady-state temperature reached during machining. Force results demonstrate that while feed rate and axial depth of cut variations cause significant changes to the process forces, cutting strategy does not. The extremely sensitive nature of this process is demonstrated through detrimental surface quality, particularly at low chip loads, due to thermal constriction occurring when trimming takes place at the tool tip.

© 2016 The Authors. Published by Elsevier B.V. This is an open access article under the CC BY-NC-ND license

(<http://creativecommons.org/licenses/by-nc-nd/4.0/>).

Peer-review under responsibility of the scientific committee of the 5th CIRP Global Web Conference Research and Innovation for Future Production

*Keywords:* CFRP, Machining, Temperature

### 1. Introduction

Secondary machining processes on moulded carbon fibre reinforced polymer (CFRP) composites continue to be vital in forming high value-added light-weight products in numerous industries from aerospace to medical devices [1].

Previous works [2-7] detail a number of CFRP-unique workpiece defect types which have been identified for the most popular CFRP machining techniques, i.e. turning, drilling, milling, trimming and alternative machining techniques such as abrasive water jetting and laser cutting. These defects include fibre linting, chemical de-bonding, fibre pull-out, uncut fibres, interply delamination and matrix pyrolysis and degradation. In addition, the ATEX classification of micro- and nano-scale CFRP particles generated during cutting introduce further challenges to the machining community. The CFRP edge trimming process has

seen significant advances in process parameter understanding and tool design to prevent many of the mechanical damage types. However, both aggressive tool wear and matrix thermal damage due to heat generated during machining remain relatively unexplored phenomena. The aim of this research is to characterise the behaviour of a number of different process-related responses to controlled changes in machining parameters.

#### 1.1. Thermal Degradation of Epoxy-based CFRP

Productivity requirements from industry are driving CFRP cutting speeds and feeds upward, ultimately increasing the potential impact of thermal energy in cut. Due to cross-linking during the polymerisation of thermoset matrix-based CFRP materials, heat exposure does not result in a 'melting' of the polymer material. Rather, temperatures from the glass

transition ( $T_g$ ) range up to the point of pyrolysis result in the formation of a structure of reduced modulus, ultimately disrupting the manner by which such thermoset-based composites undergo chip formation during cutting [8]. For temperatures beyond  $T_g$ , these thermoset materials begin to carbonize, resulting in pyrolysis and burning of the material.

The extent of heat damage on polymer composites is evaluated using mechanical, destructive analysis. Chatterjee [9] analysed polymer thermal degradation using three different techniques. Dynamic Mechanical Analysis (DMA) measured the temperature dependence of the viscoelastic modulus ( $E'$ ), loss modulus ( $E''$ ) and damping ratio. Thermogravimetric analysis (TGA) identified the thermal degradation patterns and weight loss using higher temperature ramp rates under an air environment. Dielectric analysis (DEA) allowed for the evaluation of bulk dielectric properties to infer a linear relationship with thermo-mechanical properties from DMA and TGA. The use of such techniques is extremely important for the development of an understanding of the thermo-mechanics of cutting CFRPs.

### 1.2. Temperature measurement during milling

Until recently, a major hindrance to the measurement of temperatures from a process in which the tool rotates at high-speed was an inability to access the point at which heat generation occurs in the cutting zone without intruding on the workpiece or tool geometry in some manner [10]. Since 2010, there have been a number of developments in this area. Sasahara et al. and Yashiro et al. [11, 12] investigated tool-work thermocouple, beaded thermocouples embedded in CFRP laminate and infrared thermography to obtain cutting temperatures from the process. Ueda et al. [13] developed a fibre-optics coupling which allowed a two-colour pyrometer to receive infrared radiation from the base of a cutting insert of a rotating tool. Le Coz et al. [14] used an embedded thermocouple transmitting voltage changes through a wireless acquisition system to obtain temperature information from a rotating cutting tool. A technique developed by Kerrigan and O'Donnell [15] is utilised in the current investigation. This technique employs the wireless integrated temperature (WIT) sensor method used by Le Coz et al. in combination with inverse heat transfer methods through finite element analysis to determine a quantitative temperature response during a CFRP edge trimming operation.

## 2. Experimental methodology and setup

### 2.1. Design of experiments

The experimental design incorporated a two-level full factorial approach investigating three factors. Factors were selected based upon previous experience [15, 16] in which the quality of work piece was noted to change visibly with an uncontrolled variation in these factors. The test matrix is shown in Table 1. The cutting speed and radial depth of cut (DOC) were fixed at  $250 \text{ m min}^{-1}$  and 8 mm (full slot) respectively.

Table 1. CFRP edge trimming experimental variable factors and levels.

Variable factor	Low level	High level
Feed rate ( $\text{mm min}^{-1}$ )	200	1275
Workpiece thickness / Axial depth of cut (DOC) (mm)	3	6
Central workpiece position on cutting tool axis (mm)	5	16

### 2.2. Workpiece manufacture

The dimensions of the CFRP composite flat panel used during trimming were 200 mm x 200 mm. The panel was manufactured from 12K high strength carbon / toughened epoxy prepreg. The prepreg laminae were laid up in a balanced, symmetric, quasi-isotropic arrangement of  $[0_{\text{CL}} / 0^\circ / 45^\circ / 90^\circ / -45^\circ]_s$ . A total of 10 plies were used to generate the laminate structure, with the outer two plies consisting of fibres with a dry cloth weight of 199 gsm. The remaining 8 inner plies were arranged in a symmetric arrangement consisting of fibres with a dry cloth weight of 660 gsm. The composite laminate was autoclave cured under 6.2 bar pressure using an initial cure temperature of  $90^\circ \text{C}$  for 2 hours at a ramp rate of  $0.5^\circ \text{C min}^{-1}$  with a post-cure for 15 minutes at  $200^\circ \text{C}$  followed by 8 hours at  $190^\circ \text{C}$  with a final cool down at  $3^\circ \text{C min}^{-1}$  to  $60^\circ \text{C}$ . The resulting laminate plate generated was approximately 5.2 mm thick. The fibre volume fraction for this composite plate was 55% with void content approximately  $< 1\%$ . The glass transition range, measured via DMA, was  $193^\circ \text{C}$  for this material with burning, measured via TGA, estimated to initiate at  $315^\circ \text{C}$ .

### 2.3. Experimental setup and in-process measurements

This experiment employed the setup illustrated in Fig. 1. A 3-axis Hurco VM10 CNC machine tool performed all full slot edge trimming operations. A wireless integrated temperature (WIT) sensor, employing a K-type thermocouple embedded within the cutting tool, extracted tool-side temperatures from the process. The voltage difference generated by the Seebeck effect at the thermocouple junction entered electronic modules housed within the spindle wherein cold junction referencing, amplification and filtering of the analogue voltage signal occurred. The signal was transmitted as a digital pulse code modulated (PCM) representative signal via induction from an antenna surrounding the rotating spindle. A stator positioned precisely 15 mm from the antenna transferred the signal to the data acquisition system. The information acquired was then processed using the method developed in [15] which incorporated a finite element iteration to achieve a tool cutting edge surface temperature from the embedded information acquired. The repeatability of the WIT sensor was investigated and found to be less than  $\pm 2$  percent in milling temperature measurements [14]. A FLIR A40M Researcher infrared thermal imaging camera, with a spectral range of 7 to  $13 \mu\text{m}$ , and a temperature range of 0 to  $500^\circ \text{C}$ , measured qualitative workpiece temperature changes during trimming.

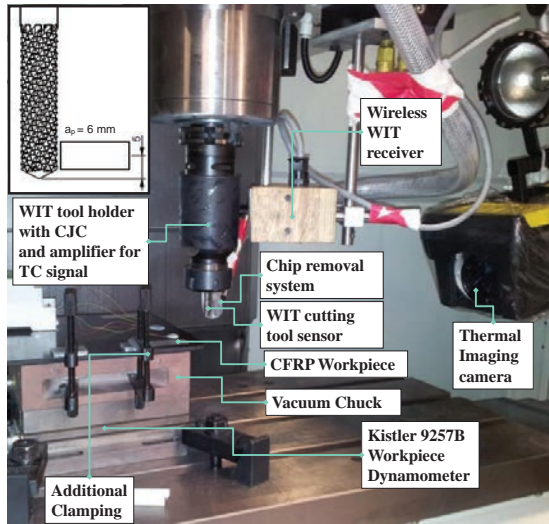


Fig. 1. Experimental setup used during full slot CFRP milling trials including thermal and force measurement sensors.

A Kistler plate dynamometer type 9257A supplied measurement data of the in-process forces following processing through charge amplifier and data acquisition system. Voltage outputs from both the WIT sensor and Kistler dynamometer were acquired simultaneously via a National Instruments PXI 1033 chassis with two NI PXI-4472B slots feeding into LabVIEW software in which calibration data was applied to convert voltages into temperature and force respectively. In addition to the sensors used, vacuum and mechanical work holding methods were employed. A local vacuum extraction chip removal system prevented exposure to CFRP particulate. This ensured repeatable, industrially relevant, stable run-to-run results. The cutting tool used in this investigation was an 8 mm diameter burr-style WC router as shown in Fig. 2. This type of tool geometry performs roughing edge-trimming operations for a variety of industrial CFRP components.

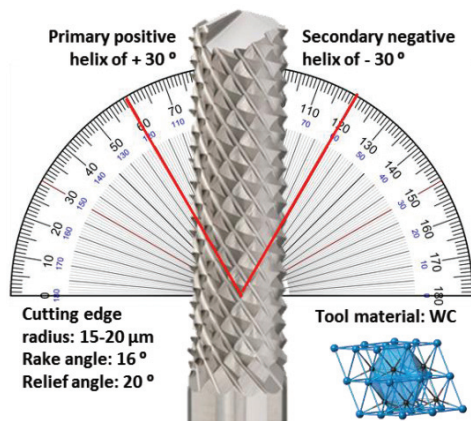


Fig. 2. Burr style router tool used for CFRP full slot edge trimming.

### 2.4. Post-machining analyses

Trimmed CFRP surface quality measurements were performed using a Mitutoyo Surftest SJ-402 stylus profilometer and a Tescan Mira variable pressure field emission scanning electron microscope (SEM) for qualitative image analysis. The stylus measurements were performed in the feed and transverse directions at 5 positions throughout the cut, as shown in Fig. 3, for each design point with the maximum  $R_y$  roughness value in all cases used for quality assessment. This represents the maximum peak-to-trough height generated on the trimmed surface.

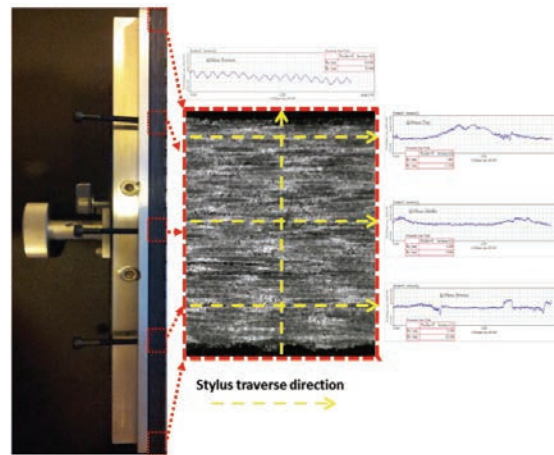


Fig. 3. Surface roughness profilometer measurement of  $R_y$  in feed and transverse directions at 5 locations on trimmed surfaces for each design point.

### 3. Results and Discussion

Fig. 4 illustrates the method used to extract cutting force information from the measured data during edge trimming. All responses measured were analysed using statistical methods incorporating Minitab software to present the information graphically. These results represent a screening result rather than a definitive surface response characterization of the behaviour of the CFRP edge trimming process.

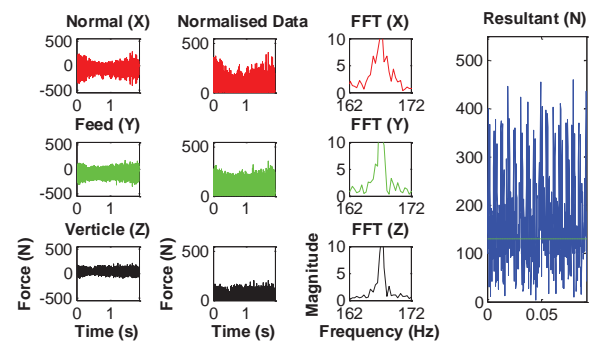


Fig. 4. Feature extraction of cutting forces via resultant force calculation and Fast Fourier Transform (FFT) to verify tooth pass frequency.

### 3.1. Cutting forces

The average resultant cutting forces for each of the runs in the design of experiment were analysed in terms of the main effects for each factor. Fig. 5 indicates that axial depth of cut (DOC),  $a_p$ , and feed rate result in statistically significant changes, with feed rate showing the largest effect.

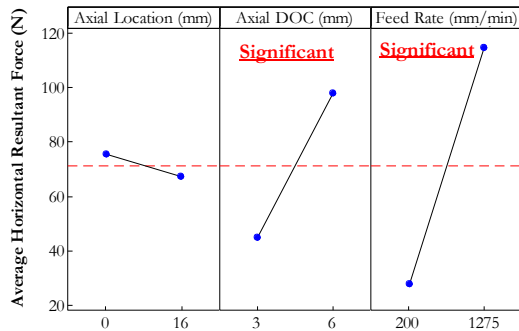


Fig. 5. Main effects plots for average resultant force.

This is potentially due to the high/low range selected for each variable with the feed rate moving from 200 mm min<sup>-1</sup> to 1275 mm min<sup>-1</sup>, which is approximately an order of magnitude change, whereas the depth of cut was doubled. The ANOVA table shown in Table 2 indicates the percentage contribution ratio (PCR) of each of the factors. This table indicates that feed rate is the dominating factor with 59% of the variance within the experiment attributable to the change in level of this factor. The depth of cut introduced a further 22% to the experimental variance with unmeasured variance contributing 19%.

Table 2: ANOVA results for average horizontal resultant forces in edge trimming.

Source	DF	SS	MS	F	P	PCR
Axial Location (mm)	1	277	277	0.45	0.513	0.00
Axial DOC (mm)	1	11350	11350	18.62	0.001	21.61
Feed Rate (mm min <sup>-1</sup> )	1	30139	30139	49.44	0.000	59.42
Error	12	7316	610			18.96
Total	15	49083				

### 3.2. Cutting tool temperatures

The tool edge temperature presents a significantly different statistical result to that from the cutting force analysis. The axial depth of cut and axial location factors produced statistically significant effects on the tool side temperature as illustrated in Fig. 6.

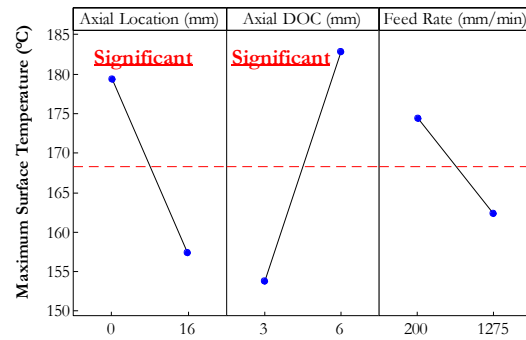


Fig. 6. Main effects plot for tool temperature.

The ANOVA table of Table 3 indicates depth of cut contributed 40% of the variance during this experiment, which is intuitive due to the additional friction associated with a larger tool-workpiece contact zone. The axial location is shown to contribute 22% of the variance which can be attributed to the thermal constriction effect seen when the tip of the tool becomes the cutting interface. The contribution of change variation of 34% of the effect on temperature indicates the potential of hidden variables within the result.

Table 3: ANOVA results for tool temperature during edge trimming tests.

Source	DF	SS	MS	F	P	PCR
Axial Location (mm)	1	1943.2	1943.2	11.47	0.005	21.91
Axial DOC (mm)	1	3370.9	3370.9	19.9	0.001	39.55
Feed Rate (mm min <sup>-1</sup> )	1	578.2	578.2	3.41	0.089	5.05
Error	12	2033	169.4			33.49
Total	15	7925.3				

### 3.3. Surface quality

The maximum Ry roughness results of the investigation are presented in Fig. 7 and Table 4. Table 4 shows that the only factor affecting surface quality was axial depth of cut. This is a counter intuitive result, as the feed rate would be expected to add variance to the results. The large error in this table points to a large amount of uncertainty in the measurement method which can be attributed to the appropriateness of both a contact stylus method and the Ry metric for assessing the surface quality of a thermally sensitive, partly polymeric, and therefore elastic, substance. In industry, the surface quality in machined components is measured using stylus method along with the Ra metric, the use of Ry in the current investigation was employed based on its ability to represent extreme changes in quality such as pitting or fibre fraying.

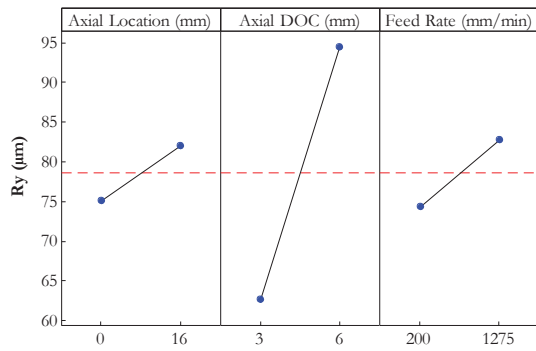


Fig. 7. Main effects plots of  $R_y$ .

Table 4. ANOVA results for  $R_y$  from edge trimming tests.

Source	DF	SS	MS	F	P	PCR
Axial Location (mm)	1	192.2	192.2	0.45	0.516	0
Axial DOC (mm)	1	4065.3	4065.3	9.48	0.01	35.96
Feed Rate (mm min <sup>-1</sup> )	1	281.6	281.6	0.66	0.434	0
Error	12	5146.8	428.9			64.04
Total	15	9686				

The resulting surfaces assessed in this research indicated an additional thermal type of damage associated with the process identifiable even by observation in the surface quality generated. Evidence of the axial tool / workpiece contact effect is shown in Fig. 8. This image indicates a fuzziness to the lower area of those surfaces, in both the 3 mm and 6 mm thick workpieces, in which the tool tip was used to perform trimming.

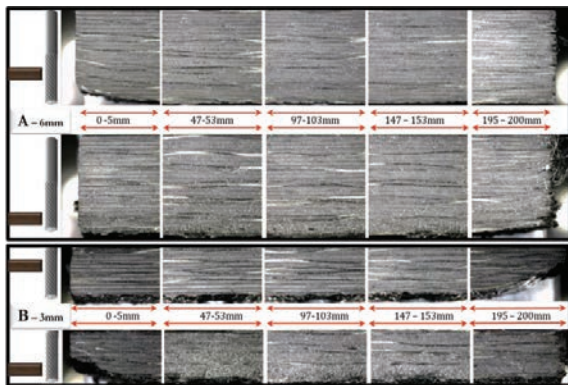


Fig. 8. Edge trimmed surfaces with indications of difference in quality due to axial variation for (a) 6mm & (b) 3mm thick samples.

Thermal constriction during heat generation occurring at the tool tip may account for this effect. In contrast, heat is able to conduct in both upward and downward directions of the rotating tool from the higher axial cutting area on the tool and no evidence is visible on the trimmed surface for these specimens in which the axial location was offset by 15 mm from the tool tip.

Closer inspection of the bottom of the CFRP workpiece trimmed using different axial positions, as shown in Fig. 9, indicates a complete lack of resin surrounding fibres in the 0° orientation when trimming with the tool tip. Such resin depletion was not observed when using a higher axial position. This is potentially an indication of the effect of the heat within the process resulting in pyrolysis of the resin in this region.

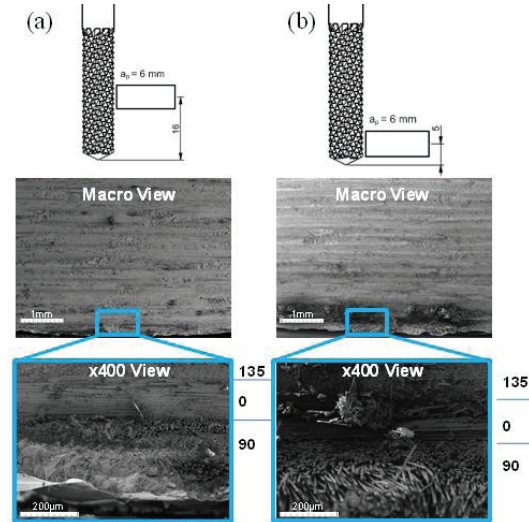


Fig. 9. SEM images of the difference in machined CFRP surface quality due to variation in axial tool engagement location for 6mm axial depth of cut for (a) 16 mm and (b) 5 mm workpiece centre offset from tool tip.

Fig. 10 indicates further evidence of a thermal effect resulting in the re-adhesion of the CFRP chip to the machined surface of the workpiece. This is due to the percentage of thermoplastic hardener within the polymer chemistry, employed to enhance the cure kinetics, which if not fully utilized during the curing process can melt and act as a binding agent at elevated temperatures. The  $T_g$  of this material was measured by DMA to initiate at 193 °C.



Fig. 10. Thermal damage in the form of chip re-adhesion to the newly trimmed CFRP surface for the case of feed rate: 200 mm min<sup>-1</sup> and axial location: workpiece at tool tip (5 mm).

### 3.4. Tool wear

The number of trimming tests performed during this experiment was minimised to prevent tool wear from influencing the statistical results. Further actions taken were

an SEM inspection and cleaning of the tool following individual trims. Presence of polymer adhered to the cutting tool was found following only those tests in which the corresponding adhesion of chip to trimmed surface was also noted as shown in Fig. 11. A typical failure mechanism in burr-style cutting tools is the accumulation of failures of individual pyramidal cutting edges that ultimately leads to catastrophic failure of the cutting tool. While there was evidence of polymer adhesion to the rake faces of the tool, this was removed between cutting operations. There was no evidence of pyramidal failures in the current investigation. Thus, tool wear was determined to be a non-factor in the results presented herein.

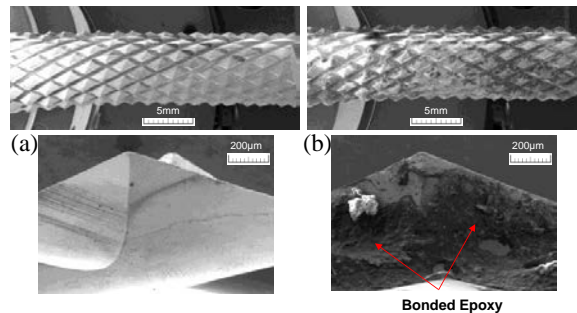


Fig. 11. SEM images of the cutting tool taken (a) pre- and (b) post-machining of a single 200 mm trimmed edge.

#### 4. Conclusions

- This investigation demonstrates the usefulness of measuring a number of responses, both direct, such as surface quality, and indirect, such as force and temperature, in order to develop an understanding of CFRP edge trimming.
- While the key variable in the vast majority of machining applications is the overall surface quality as this relates to the performance of the component in some way, the usefulness of in-process responses should not be overlooked. This is particularly relevant of in-process temperatures for polymeric composite edge trimming applications, which have demonstrated an ability to identify potential damage not detected when using conventional machining process monitoring methods.
- There is a relationship between temperatures generated and the overall quality of the machined workpiece. In addition, the use of tool-side temperature response has provided insight into comparative effect of a variety of factors including feed rate, depth of cut and axial position of the tool in cut.
- The feed rate accounted for approximately 60% of the energy input in the cutting operation, as indicated by the cutting force statistics, whereas the axial depth of cut accounted for 20% and axial tool position had no effect for those parameter levels tested.
- The energy out of the tool-side part of the system, represented by the temperature, appears to tell a very different story in which the axial depth of cut accounts for

40% of the variance in the experiment with axial position and feed rate accounting for 20% and 5% respectively.

#### Acknowledgements

The authors would like to thank the Irish Research Council for Science, Engineering and Technology (IRCSET) and the EU FP7 funding program – Adaptive Control for Metal Cutting (ADACOM) for the financial support within this project.

#### References

- [1] M'Saoubi, R., D. Axinte, S.L. Soo, C. Nobel, H. Attia, G. Kappmeyer, . . . W.-M. Sim, High performance cutting of advanced aerospace alloys and composite materials. *CIRP Annals - Manufacturing Technology*, 2015. 64(2): p. 557-580.
- [2] Davim, J.P. and P. Reis, Damage and dimensional precision on milling carbon fiber-reinforced plastics using design experiments. *Journal of Materials Processing Technology*, 2005. 160(2): p. 160-167.
- [3] Lasri, L., M. Nouari and M.E. Mansori, Wear resistance and induced cutting damage of aeronautical FRP components obtained by machining. *Wear*, 2011. 271(9-10): p. 2542-2548.
- [4] Sheikh-Ahmad, J., N. Urban and H. Cheraghi, Machining Damage in Edge Trimming of CFRP. *Materials and Manufacturing Processes*, 2012. 27(7): p. 802-808.
- [5] Haddad, M., R. Zitoune, H. Bougherara, F. Eyma and B. Castanié, Study of trimming damages of CFRP structures in function of the machining processes and their impact on the mechanical behavior. *Composites Part B: Engineering*, 2014. 57: p. 136-143.
- [6] Haddad, M., R. Zitoune, F. Eyma and B. Castanie, Study of the surface defects and dust generated during trimming of CFRP: Influence of tool geometry, machining parameters and cutting speed range. *Composites Part A: Applied Science and Manufacturing*, 2014. 66: p. 142-154.
- [7] Sheikh-Ahmad, J.Y., *Machining of Polymer Composites*. 2009, New York: Springer.
- [8] Santhanakrishnan, G., R. Krishnamurthy and S.K. Malhotra, High speed steel tool wear studies in machining of glass-fibre-reinforced plastics. *Wear*, 1989. 132(2): p. 327-336.
- [9] Chatterjee, A., Thermal Degradation Analysis of Thermoset Resins. *Journal of Applied Polymer Science*, 2009. 114: p. 1417-1425.
- [10] Davies, M.A., T. Ueda, R. M'Saoubi, B. Mullany and A.L. Cooke, On The Measurement of Temperature in Material Removal Processes. *CIRP Annals - Manufacturing Technology*, 2007. 56(2): p. 581-604.
- [11] Hashish, M. Trimming and drilling of CFRP components. in *SAMPE Tech Seattle 2014 Conference*. 2014. Soc. for the Advancement of Material and Process Engineering.
- [12] Yashiro, T., T. Ogawa and H. Sasahara, Temperature measurement of cutting tool and machined surface layer in milling of CFRP. *International Journal of Machine Tools and Manufacture*, 2013. 70: p. 63-69.
- [13] Ueda, T., M. Sato, A. Hosokawa and M. Ozawa, Development of infrared radiation pyrometer with optical fibers—Two-color pyrometer with non-contact fiber coupler. *CIRP Annals - Manufacturing Technology*, 2008. 57(1): p. 69-72.
- [14] Le Coz, G., M. Marinescu, A. Devillez, D. Dudzinski and L. Velnom, Measuring temperature of rotating cutting tools: Application to MQL drilling and dry milling of aerospace alloys. *Applied Thermal Engineering*, 2012. 36(0): p. 434-441.
- [15] Kerrigan, K. and G.E. O'Donnell, Temperature Measurement in CFRP Milling using a Wireless Tool-Integrated Process Monitoring Sensor. *International Journal of Automation Technology*, 2013. 7(6): p. 742 - 750.
- [16] Kerrigan, K., J. Thil, R. Hewison and G.E. O'Donnell, An Integrated Telemetric Thermocouple Sensor for Process Monitoring of CFRP Milling Operations. *Procedia CIRP*, 2012. 1(0): p. 449-454.